中國機械工程學刊第四十一卷第五期第 527~538 頁(民國一百零九年)
Journal of the Chinese Society of Mechanical Engineers, Vol.41, No.5, pp 527~538 (2020)

Simulation Model and Equations for Fabrication of Connecting Straight Line Segment with Arc Nanochannel to the Expected Width and Expected Depth and Verification of Atomic Force Microscope Fabrication Experiment

Zone-Ching Lin * and Ying-jie Qin **

Keywords: Atomic Force Microscopy, arc, offset fabrication method of two cutting passes, expected width, expected depth

ABSTRACT

This paper proposes a simulation model and equation for fabrication of a nanochannel trapezium groove that has straight line segment connected with arc of $\frac{1}{4}$ circle, to the expected width and expected depth, and uses the simulation model to obtain the total offset amount of probe, the number of cutting passes on each cutting layer, the probe offset amount between two cutting passes, equation of protruding height value on the bottom, downward force of each cutting pass on each cutting layer, number of near arc of $\frac{1}{4}$ circle shaped tiny line segments and length of each tiny line segment. After that, the paper conducts atomic force microscopy (AFM) experiment of integrated straight line segment and arc of $\frac{1}{4}$ circle fabrication of nanochannel trapezium groove, with fabrication to the expected width and expected depth. Finally, the fabrication results obtained from AFM experiment are measured, verifying that the simulation model and equation proposed by the paper are feasible and acceptable. The paper also derives a straight line equation required for measurement of the cross-section of the tiny line segments of near arc of $\frac{1}{4}$ circle during measurement, and the method for measurement of cross-section. To sum up, the abovementioned simulation model and equation, and the AFM experiment and measurement method proposed in this paper have academic innovativeness and application value.

Paper Received August, 2020. Revised September, 2020. Accepted October, 2020. Author for Correspondence:Zone-Ching Lin.

* *Professor, Department of Mechanical Engineering, National Taiwan University of Science and Technology, No.43, Keelung Rd., Sec.4, Da'an Dist., Taipei City 10607, Taiwan,*
email: zclin@mail.ntust.edu.tw.
** *Graduated Student, Department of Mechanical Engineering, National Taiwan University of Science and Technology, No.43, Keelung Rd., Sec.4, Da'an Dist., Taipei City 10607, Taiwan,*
email: m10703236@mail.ntust.edu.tw

INTRODUCTION

Many scholars once studied the measurement and machining application of AFM. Nanjo et al.(2003) considered the sharp tip of TM-AFM probe as a perfect sphere to carry out simulated small-sphere scanning on an ideal plate under a fixed setpoint value. Lüben et al.(2004) saw probe tip as a perfect sphere, and used contact mode AFM to explore the probe deflection and vertical pressure on a quartz plate. AFM is a tool that can be used not only to directly observe the microscopic appearance of a substance's surface, but also to analyze the chemical, physical and mechanical properties of a substance's surface, and even can control a single atom, and make AFM itself become an important equipment for fabrication of tiny parts and microstructures. The main reason for the use of AFM probe tip to conduct mechanical cutting was that due to the change of action force between probe tip and sample, applying sufficient downward force on the probe tip could make the probe tip press down onto the surface of object. With the movement of the probe tip, cutting can be carried out to form specific geometric patterns, and thus fabricating specific nanostructure. Therefore, for fabrication of nanoscale microstructures, not only the high-cost electronic beam or ionic beam fabrication methods can be used, AFM can also be applied to nanolithography and nanoscale cutting. It was proved by the related scholars that applying AFM probe as a fabrication cutting tool to carry out mechanical cutting was a quite useful technique in fabrication of nano-microstructures, such as semiconductor, optoelectronic components and metallic surface (2008. Fang et al. (2000) used AFM probe to conduct nano-scratching experiments of silicon (Si) substrate coated with crystal-free aluminum (Al.) film. Experimental results showed that scratch depth deepened with the increase of probe tip load and scribing cycles. Besides, the effects of downward force of the cutting tool of probe were most obvious. Schumacher et al. (2000) used AFM to carry out mechanical cutting on the surface of heterogeneous structures of GaAs/AlGaAs, and then fabricated a single-electron transistor. Yongda et al. (2007) directly used AFM to construct a system similar to computer numerical control (CNC) fabrication system, and took AFM probe as a cutting tool to carry out scratching of micro-nanostructures on the surface of silicon wafer deposited with copper film. Wang et al. (2010) used AFM to fabricate nanochannel on the surface of silicon oxide, and explored through experiments how downward was related to cutting speed and cutting depth. The experiment of scratching Si wafer by AFM cutting tool of probe done by Tseng (2010) also showed that the depth and width of the scratched groove increased with the increase of downward force and scratch cycles of probe. Lin and Hsu (2012) used the theory of specific down force energy (SDFE) to explore the V-shaped groove produced on the sapphire being cut at different downward forces, and explore the method of reaching the expected fabrication depth with the fewest cutting passes when fabricating a V-shaped groove on each cutting layer for a single cutting pass only. Cardoso et al. (2018) used the polydimethylsiloxane (PDMS) microfluidic system, which is manufactured by the copy mode of the premade SU-8 model that was obtained by using lithography, to perform highly effective cleaning of magnetic nanoparticles. Teerasong and McClain (2011) used photolithographic technology to establish microfluidic device. The microfluidic channel in this literature is a nanochannel combining straight line segment with $\frac{1}{4}$ arc of circle.

Therefore, this paper takes the microfluidic channel of Teerasong and McClain(2011) for reference, and carries out planning of a path to connect straight line segment and arc fabrication. None of the above literatures mention the simulation model and equation proposed by this paper, which uses AFM for fabrication of a nanochannel trapezium groove, through connection of straight line segment with arc of $\frac{1}{4}$ circle fabrication, to the expected width and expected depth. The paper also conducts verification of the experiment using AFM to fabricate a nanochannel trapezium groove.

EXPERIMENTAL EQUIPMENT AND SPECIFIC DOWN FORCE ENERGY MODEL AND EXPERIMENTAL METHOD

Introduction of Experimental Equipment

The AFM machine used in the study is Veeco Instruments Inc.'s AFM machine of Dimension 3100 (D3100), which is equipped at the laboratory of Tungnan University; and the material used in the paper's experiments is silicon substrate with diameter 2 inches and thickness 254-304μm, which was provided by Ample Gola International Co., Ltd. The probe used in experiments is the diamond-coated DT-NCHR probe produced by NanoSensors Inc. The thickness of the diamond coating is around 100nm, and the probe tip is like a semi-sphere with a spherical radius of around 150nm. Therefore, when this probe is used for fabrication of silicon wafer, the probe tip is just like a semispherical cutting tool. The spring constant k_v of the probe provided by the manufacturer is 42 N/m, and its resonance frequency f_v is 320 kHz. In order to obtain a more accurate spring constant k_r of probe, the paper firstly uses tapping mode AFM to find the actual resonance frequency f_r of probe for experiments. It obtains the value of f_r is 309.6kHz Besides, since the spring constant k_r of probe in the experiments can be obtained from the equation $k_r = (f_r^2 \times k_v)/f_v^2$, the actual spring constant k_r of probe in the experiments can be acquired from the resonance frequency f_v and spring constant k_v of probe provided by the manufacturer. It obtains the value of k_r is 39.3kHz

Measurement Method of the Downward Force of AFM Probe

For the nanofabrication way by AFM contact mode, the probe firstly presses down into the workpiece. This research uses force-distance curve for measuring downward force. The force-distance curve explains the relationship between setpoint value and offset amount of the probe cantilever. Before conducting the experiment, the paper firstly sets different setpoint values for AFM machine under the contact model, and then substitute the offset amount d of probe cantilever measured by different setpoint values in equation (1) to acquire the corresponding downward force value F_d of the setpoint. In equation (1), k_r is the spring constant of probe.

$$F_d = k_r d \tag{1}$$

SDFE Theoretical Model and SDFE Calculation Method

This research applies specific down force energy (SDFE) as the fixed value, and uses AFM experiment to calculate the SDFE of the fabricated single-crystal silicon substrate. As downward force energy is produced from pressing downward into the workpiece for a certain depth, fabrication is carried out in cutting direction. The mechanism that the workpiece is being fabricated is just the moving and removal of atomic particles, and this is a volume change mode. SDFE is defined as follows: Let the downward force of fabrication applied by the cutting tool of probe onto the workpiece multiply the power of cutting depth to produce energy; and then divide such energy by the volume removed from the workpiece by the cutting tool due to downward force. The equation of SDFE is shown in equation (2) (Lin and Hsu, 2012):

$$\text{SDFE(specific down force energy)} = \frac{F_d \times \Delta d_n}{\Delta V_n} \quad (2)$$

Here, F_d denotes the downward force applied by cutting tool onto the workpiece; Δd_n denotes the increased cutting depth for cutting at the cutting pass on the n^{th} layer; and ΔV_n denotes the volume removed from the workpiece at the n^{th} cutting pass. Since the volume removed from the workpiece by downward force changes with the increase of fabrication depth, ΔV_n is the function of cutting depth Δd_n.

From the moving of cutting tool to the fabrication of groove, the depth in the middle area gradually inclines to be at a fixed cutting depth. As to the volume removed by downward force after moving of cutting tool, due to fabrication in the abovementioned process, the volume of the distance of the radius R behind the cap of the workpiece being cutted in by the probe in advancing direction has been removed. Therefore, at this moment, the removed volume at the 1st cutting pass on the 1st cutting layer is half of the cap volume under the cutting depth Δd_1, and the removed volume ΔV_1 is shown as follows:

$$\Delta V_1 = \frac{1}{2}\pi \Delta d_1^{\,2}\left(R - \frac{\Delta d_1}{3}\right) \quad (3)$$

where R denotes the radius of the tip of the cutting tool of probe; and Δd_1 denotes the cutting depth of the 1st cutting pass on the 1^{st} cutting layer.

As to the volume removed by downward force at the 1st cutting pass on the 2nd cutting layer, since the groove is removed at the 1st cutting pass on the 1st cutting layer, the removed volume is just like an arc wedge. Therefore, for the geometric shape of cutting tool and the cutting depth, the paper uses CATIA's CAD software to make a solid model in order to carry out simulation and calculation of the volume removed by the downward force at 1st cutting pass on the 2nd cutting layer.

This study uses the downward forces 30.23 μN and 40.21 μN respectively to cut the silicon substrate by a probe of AFM machine, then measures the cutting depth Δd_1 and calculates the removed volumes ΔV_1 by CAD software. After that, this study substitues the downward forces, cutting depths Δd_1 and removed volumes ΔV_1 into the equation (2) of SDFE. Finally, this study obtain the SDFE value of the silicon substate is 0.01775 $\mu N \cdot nm / nm^3$.

OFFSET FABRICATION METHOD OF TWO CUTTING PASSES FOR MACHINING NANOCHANNEL TRAPEZIUM GROOVE

The study's offset fabrication method of two cutting passes for machining nanochannel trapezium groove is explained as follows: First of all, it is set that under a fixed downward force on each cutting layer, the cutting depth at the 1st cutting pass is firstly cut. After that, the probe is offset rightwards to cut the workpiece at the 2nd cutting pass on this cutting layer with the different downward force. During this time the cutting depth at the 2nd cutting pass on this cutting layer has the same cutting depth as the 1st cutting pass. In this way, between the shape of nanochannel the cut cross-section before probe offset and the shape of the cut cross-section of nanochannel trapezium groove bottom at the two cutting passes after probe offset, there is a protruding height value H on the bottom, as shown in Figure 1.

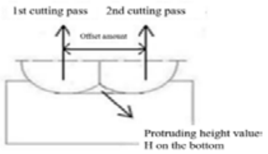

Figure 1 Schematic diagram of protruding height value H on the bottom of trapezium groove between two cutting passes

If this protruding height value H on the bottom of nanochannel trapezium groove exceeds the set convergence value of protruding height value on the bottom, the probe should be offset step by step to carry out cutting. After step-by-step offset of the probe, the protruding height value H on the bottom at the two cutting passes of fabrication is made to converge to within a range. In order to make the nanochannel trapezium groove's bottom on straight-line nanochannel have a result closer to a plane after cutting at the bottom, this research sets the numerical value of the protruding height value on the bottom to be a numerical value of the surface roughness of single-crystal silicon substrate at below 0.54nm. Right now, it is supposed that the probe offset amount required for cutting of nanochannel trapezium groove has been reached. During this time, after the probe is offset, substitute the SDFE value obtained from AFM experiment in SDFE equation (2). Since ΔV_n in equation (2) is the function of Δd_n, which is the same cutting depth at the 1st cutting pass on this cutting layer. Since the radius of AFM probe has been known, CAD software can be used to find ΔV_n. After inverse induction from equation (2), the required downward force for fabrication nanochannel trapezium groove at the 2nd cutting pass on this cutting layer after probe offset can be acquired.

If it is required to simulate the nanochannel trapezium groove that uses a greater depth after the 2nd cutting layer, then under the preset cutting depth on the 2nd cutting layer, volume is removed during cutting on the 1st cutting layer, and the removed volume is just like an arc wedge. Therefore, the paper uses CAD software to calculate the removed volume. Similarly, using SDFE equation (2) can obtain the downward force required for the cutting pass on the 2^{nd} cutting layer. Therefore, the paper takes this concept to establish this cutting layer that has the same cutting depth, and to simulate the required downward force of each cutting pass on each cutting layer.

If it is required to increase the width of nanochannel trapezium groove on straight-line nanochannel with the same cutting depth on this cutting layer, then use the same probe offset amount of the two adjacent cutting passes on this cutting layer. Offset the probe rightwards, and calculate the required downward force. Then the trapezium groove pattern on nanochannel required on this cutting layer that has three cutting passes can be simulated.

ESTABLISHMENT OF FABRICATION METHOD OF NANOCHANNEL TRAPEZIUM GROOVE OF STRAIGHT LINE SEGMENT TO THE EXPECTED WIDTH AND EXPECTED DEPTH

This research uses the above offset fabrication method of two cutting passes. The study further applies the fabrication method of trapezium groove on straight line segment nanochannel to the expected width and expected depth. This method can decide the required number of cutting passes n for fabrication of nanochannel trapezium groove to the expected depth and expected width, total offset amount P_{total} of probe among cutting passes, probe offset amount P_n between two adjacent cutting passes, and the protruding height value H on the bottom produced between two adjacent cutting passes.

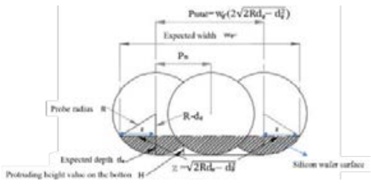

Figure 2 Schematic diagram of geometric relationship in fabrication of nanochannel trapezium groove on straight line segment to the expected width and expected depth (3 cutting passes)

First of all, set the numerical values of the expected width and expected depth for fabricating to the last cutting layer, as shown in Figure 2. In Figure 2, d_e denotes the expected depth for fabricating to the last nanochannel trapezium groove; w_e denotes the expected width for fabricating to the last nanochannel trapezium groove; P_{total} denotes the total offset amount of probe; P_n denotes the probe offset amount at two adjacent cutting passes; H denotes the protruding height value on the bottom; and z denotes the horizontal distance from the center of probe to the connected place between probe and the edge of trapezium groove. As the probe tip radius R is known to be 150nm, the equation of Pythagorean theorem can be used to derive equation z in Figure 2 as follows:

$$Z = \sqrt{2Rd_e - {d_e}^2} \tag{4}$$

From Figure 2, it can be seen that there is z by both the left and right sides at the farthest cutting pass, so that $2z = 2\sqrt{2Rd_e - {d_e}^2}$. In order to obtain the required total offset amount of probe, equation (5) of total offset amount of probe P_{total} can be derived from Figure 2 as follows:

$$P_{total} = w_e - (2\sqrt{2Rd_e - {d_e}^2}) \tag{5}$$

As seen from equation (5), when the last expected depth d_e and expected width w_e of nanochannel trapezium groove have been known, the total offset amount of P_{total} probe can be acquired from equation (5).

As known from Figure 2, H is the protruding height value on the bottom of nanochannel trapezium groove produced between two adjacent cutting passes; P_n is the probe offset amount between two adjacent cutting passes; and the n in P_n represents the number of cutting passes on each cutting layer. If there are two cutting passes only, the n in P_n is 2, and $P_{total} = P_2$. Therefore, from Figure 2, P_n and H equations can be derived and expressed as equations (6) and (7) as follows:

$$P_n = \frac{P_{total}}{n-1} \tag{6}$$

$$H = R - \sqrt{R^2 - (\frac{P_n}{2})^2} \tag{7}$$

From equation (5), we can calculate the required total offset amount P_{total} of probe for fabrication of nanochannel trapezium groove to the expected width and expected depth. If each cutting layer is divided into n cutting passes for cutting, equation (5) can be used to calculate the total offset amount P_{total}. According to equation (6), after dividing by (n-1), we can calculate the probe offset amount P_n between two adjacent cutting passes required for reaching the expected width and expected depth of nanochannel trapezium groove. After we have obtained the probe offset amount P_n between two adjacent cutting passes on each cutting layer, we also have to substitute this P_n value in equation (7) to calculate the protruding height value H on the bottom, and then observe the selected number of cutting passes, and check whether the protruding height value H on the bottom has exceeded the convergence value 0.54nm. If the calculated protruding height value H on the bottom has exceeded the convergence value 0.54nm, we can increase one more cutting pass, and substitute the number of cutting passes n, with a cutting pass additionally increased, in equation (6). Calculate the required probe offset amount P_n, and then observe again whether the protruding height value H on the bottom still exceeds 0.54nm.

If the protruding height value H on the bottom has not exceeded the convergence value 0.54nm, the number of cutting passes n for the new set cutting passes is the required number of cutting passes on each cutting layer.

ESTABLISHMENT OF SIMULATION MODEL FOR CUTTING OF NANOCHANNEL THAT CONNECTS STRAIGHT LINE SEGMENT WITH ARC SEGMENT FABRICATION TO THE EXPECTED WIDTH AND EXPECTED DEPTH

In the connection and integration process, for the simulated cutting model of nanochannel that connects straight line segment connected with arc of $\frac{1}{4}$ circle segment fabrication to the expected width and expected depth, since the fabrication process from straight line segment to the arc segment is continuous, the downward force, offset amount, number of cutting passes and number of cutting layers used for arc segment fabrication at each cutting pass are the same as those of straight line segment fabrication. Since such fabrication is continuous, when the cutting tool works from straight line segment to are segment fabrication, an equation of the arc has to be decided first. Therefore, the equation of an ideal arc segment at each cutting pass has to be derived first.

However, the smallest resolution achieved in fabrication by AFM machine is 1nm only. Thus, we have to obtain multiple tiny straight lines from different ideal arcs and connect these tiny straight lines to achieve a near arc of $\frac{1}{4}$ circle. The method of obtaining tiny straight lines for a near arc of $\frac{1}{4}$ circle is through a chord height tolerance equation, which makes the chord height tolerance less than 0.5nm.

Establishment of Arc Equation for the Ideal Arc Fabrication

Regarding the paper's nanochannel that connects straight line segment with arc fabrication, the arc is an arc of ¼ circle formed by its intersection with two straight line segments, as shown in Figure 3. In Figure 3, (x_0, y_0) are the coordinates of the center of the arc; and r is the radius of the arc. Point $P(x_1, y_1)$ and point $P(x_2, y_2)$ in Figure 3 are the coordinates of the two points where the two straight lines intersect with the arc of ¼ circle

The steps for establishment of arc equation for the ideal arc fabricated are shown below.

Therefore, the equation for the arc adopted by the paper's ideal arc of ¼ circle is as follows:

$$(x-x_0)^2 + (y-y_0)^2=r^2 \tag{8}$$

Here, (x_0,y_0) are the coordinates for the position of the center; and r is the radius of the arc.

Hence, using the practice of Figure 3, the position for the center of the arc of ¼ circle can be planned to be (x_0, y_0). The coordinates, $P(x_1, y_1)$ and $P(x_2,y_2)$, of the points where two straight line segments intersect with the arc, as well as the radius r can be substituted in equation (8).

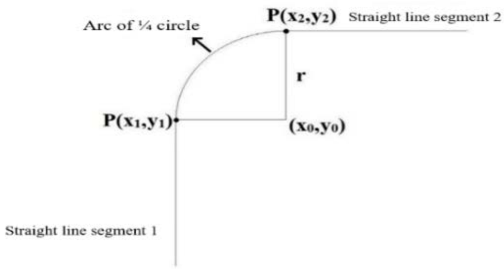

Figure 3 Schematic diagram of connection of straight line segments with the arc of ¼ circle

Establishment of Equations for Arc of $\frac{1}{4}$ circle at Different Cutting Passes after Offset

After offset, establish an equation for the arc at the 2nd cutting pass. The offset amount during offset this time is the simulated offset amount of straight line segment fabrication mentioned in the step aforesaid. After that, according to the probe offset amount between two cutting passes for the straight line segment at the 2nd cutting passes, we carry out offset for the two control points of the 1st arc already established, and then use the positions of the two control points $P_2(x_3, y_3)$ and $P_2(x_4, y_4)$ after offset to establish an arc equation at the 2nd cutting pass. Right now, the arc radius r_2 at the 2nd cutting pass is $r_2=(r-P_n)$, where r is the radius of arc of ¼ circle at the 1st cutting pass, as shown in Figure 3 and Figure 4.

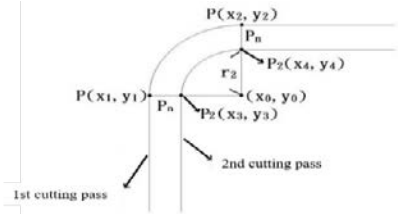

Figure 4 The arc radius r_2 at the 2nd cutting pass is $r\text{-}P_n$

The established concept of the arc of ¼ circle at the 3rd cutting pass is based on the control point of the arc at the 2nd cutting pass. The above way is used to calculate the control point of the arc at the 2nd cutting pass; and the method of obtaining equation is used to obtain the control point and equation of the arc at the 3rd cutting pass. If it is required to calculate the equation of the arc at the 4th cutting pass, the above steps can be followed to make calculation.

Establishment of Tiny Straight Line Segments for an Arc of $\frac{1}{4}$ Circle

When multiple tiny straight line segments are used for approximation to fabrication of an arc of near-¼ circle, the chord height tolerance (being the vertical distance between the tiny straight line segments of the near-arc and the ideal arc) is used by this research to serve as a reference for judgment of difference in shape between the path of tiny straight line segment and the arc of ¼ circle. Focusing on the method that an arc of ¼ circle uses tiny straight line segments for approximation to fabrication of a near arc curve, the equation of chord height tolerance according to reference (Yeh and Hsu, 2002) is expressed as equation (9).

The equation for calculation of chord height tolerance is as follows:

$$d_{\text{all max}}=\rho_i-\sqrt{\rho_i-\left(\frac{L_i^{Arc}}{2}\right)^2} \tag{9}$$

where: $d_{all\ max}$ denotes the supposed permissible maximum chord height tolerance. The smaller this value, the nearer the fabrication path approximates to the fabricated arc.

L_i^{Arc} denotes the length of the i^{th} tiny straight line segment obtained from calculation by near arc of $\frac{1}{4}$ circle of tiny straight line segments. Therefore:

$$L_i^{Arc}=2\sqrt{\rho_i-(\rho_i-d_{\text{all max}})^2} \tag{10}$$

From equation (10), the length L_i^{Arc} of the i^{th} tiny straight line segment of the near $\frac{1}{4}$ arc of tiny straight line segments can be obtained. And from this length, the position of the $(i+1)^{th}$ intersection point Q_{i+1}^{Arc} between the i^{th} tiny straight line segment and the arc can be calculated. Therefore, the length L_i^{Arc} can be used to estimate the $(i+1)^{th}$ intersection point Q_{i+1} on the arc. Since the arc at the farthest periphery has the greatest radius, when it gets closer to the inner side, the acquired radius of arc would be smaller, and thus the calculated chord height tolerance would also be smaller. Therefore, we start calculation from the arc at the farthest periphery so as to more conveniently control our expected chord height tolerance.

Besides, the radius of curvature ρ_i of the arc of ¼ circle is just the radius r of its arc. Thus, the ρ_i in the chord height tolerance equation (9) is expressed as the radius r, and the equation is changed to be:

$$d_{\text{all max}}=r-\sqrt{r-\left(\frac{L_i^{Arc}}{2}\right)^2} \tag{11}$$

And the equation (10) of the length of the i^{th} tiny straight line segment L_i^{Arc} is changed to be:

$$L_i^{Arc}=2\sqrt{r-(r-d_{\text{all max}})^2} \tag{12}$$

$d_{\text{all max}}$ and L_i^{Arc}, in relation to equation (11) and equation (12), are expressed in the schematic diagram of Figure 5.

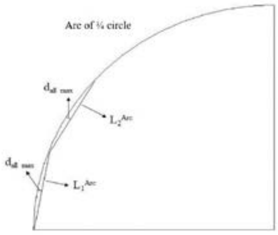

Figure 5 Schematic diagram of the length of the tiny straight line segment L_i^{Arc} of the near-arc of the arc of ¼ circle and the chord height tolerance $d_{\text{all max}}$

The paper's $d_{\text{all max}}$ is supposed to be 0.5nm; its expected width is greater than 200nm; and its expected depth is less than 100nm. But the last chord length L_f^{Arc} on the arc of ¼ circle is obtained by coping with the last control point $P(x_2, y_2)$ of the arc of ¼ circle. Therefore, when the chord length L_f^{Arc} obtained from the previous point and the last control point $P(x_2, y_2)$ is substituted in equation (11), we can calculate the last $d_{f\ max}$, i.e. $d_{f\ max}=r-\sqrt{r-\left(\frac{L_f^{Arc}}{2}\right)^2}$,which can be known to be smaller than 0.5nm or not.

SIMULATION RESULTS AND VERIFICATION STEPS OF MEASUREMENTS IN AFM FABRICATION EXPERIMENT

The verification steps for measurement of the results of simulation established by this research and the results of AFM fabrication experiment are explained as follows:

1. Regarding verification of the simulation model of straight line segment fabrication, we use the simulated result of straight line segment fabrication to carry out verification. Take a cross-section from

the fabricated straight line segment to carry out measurement.

2. For the first example of measurement, the measured cross-section of the ideal arc of ¼ circle is the position of straight line formed by connecting the first control point $P(x_1, y_1)$ of the arc of ¼ circle at the 1st cutting pass with the first control point $P_2(x_3, y_3)$ of the arc of ¼ circle at the 2nd cutting pass. Since two points can determine a line, we can suppose that the equation of its straight line is $y = ax+b$. Substitute the two control points $P(x_1, y_1)$ and $P_2(x_3, y_3)$ with their positions known in the simultaneous equations, and then the straight line equation of the measured cross-section can be acquired. This straight line epuation of measured cross-section is the first measured cross-section as shown in Figure 6.
3. Take the points where the tiny line segments of the near-arc at the 1st cutting pass intersect with the arc of ¼ circle as well as the center of the arc of ¼ circle. For the obtained coordinates of this intersection point and the center, use the straight line equation achieved in Step 2 to form simultaneous equations. Then the straight line equation of another measured cross-section can be obtained. This is the second measured cross-section as shown in Figure 6. After that, confirm whether the two points that the straight line of the measured cross-section intersects with the tiny straight line segments at the 1st cutting pass and that with the tiny straight line segments at the 2nd cutting pass are both on the tiny straight line segments of the arc of near-¼ circle at the 1st cutting pass and the tiny straight line segments at the 2nd cutting pass, so as to avoid an excessively great difference between the compared position and the calculated position during the comparison to be subsequently made.
4. Calculate again the position of the intersection point between the straight line equation of the measured cross-section and the tiny straight line segments of the arc of near-¼ circle at the 1st cutting pass as well as the position of the intersection point between that and the tiny straight line segments at the 2nd cutting pass. Then, calculate the distance between the positions of these two intersection points. Such a distance is just the offset amount of the arc of near-¼ circle of the two tinystraight line segments at the 1st cutting pass and the 2nd cutting pass.
5. Carry out simulation according to different fixed downward forces set for tiny straight line segments at different cutting passes during straight line fabrication as well as the offset amount of two tiny straight line segments calculated in Step 4. Then the simulated width, depth and protruding height value of the cross-section at the measurement positions of two tiny straight line segments can be acquired. They are compared to the width, depth and protruding height value obtained from the cross-section at the same measurement positions of the AFM experiment. Then we can achieve the difference between the simulation result and the AFM experimental result of the arc of near-¼ circle.
6. Following the similar practice in Step 3, at the position of around the middle of a certain tiny straight line segment of the arc of near-¼ circle at the 1st cutting pass, just at above the position roughly close to the maximum chord height tolerance value, select a point on the first arc of ideal near-¼ circle, and use the center of the arc of ¼ circle. Using the method in Step 2, calculate the straight line equation. The straight line obtained from this straight line equation intersects with a certain tiny straight line segment of the arc of near-¼ circle at the 2nd cutting pass. This straight line equation is just the equation of straight line of the cross-section to be measured by us. This is the third measured cross-section as shown in Figure 8. This equation and the straight line equations of tiny straight line segments of the near-arc at the 1st cutting pass and the 2nd cutting pass calculated in Step 3 form simultaneous equations. After solving them, we can obtain the positions of the intersection points where the tiny straight line segments of the arc of near-¼ circle at the 1st cutting pass and the tiny straight line segments at the 2nd cutting pass respectively intersect with the straight line equation of the measured cross-section. Then, use Step 4 to calculate the distance between the positions of the two intersection points obtained at the two cutting passes. Such a distance is just the offset amount of two intersection points where two tiny straight line segments at the 1st cutting pass and the 2nd cutting pass intersect with the straight line equation of the measured cross-section. After that, this offset amount is used to carry out simulation, and then we can achieve the width, depth and protruding height value simulated on the cross-section at the two cutting passes between two tiny straight line segments at the 1st cutting pass and the 2nd cutting pass at around the middle positions of the arc of near-¼ circle at the 1st cutting pass and the the 2nd cutting pass. These achieved results are compared to the width, depth and protruding height value of the cross-section measured in the AFM experiment that measures the same measured cross-section. Then the difference between the simulation results and the AFM experimental results can be obtained.
7. If the value of difference between the simulation results and the experimental results is small, it can be proved that the simulation model of nanochannel trapezium groove with straight line segment connecting with arc of $\frac{1}{4}$ circle segment fabrication to the expected width and expected depth, as established by the paper, is reasonable.

Figure 6 shows the schematic diagram of the measured cross-section mentioned in the above verification steps of measurement. There are three measured cross-sections shown in Figure 6.

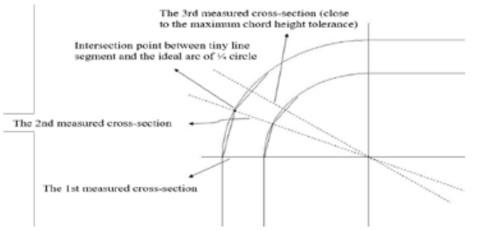

Figure 6 Schematic diagram of the measured cross-section

SIMULATION RESULTS AND EXPERIMENTAL VERIFICATION

Exploration of Simulation of Straight Line Segment and Arc Segment to the Expected Width and Expected Depth

The shape of nanochannel trapezium groove that integrates straight line segment with arc of $\frac{1}{4}$ circle segment fabrication, as explored in the paper (Teerasong and McClain, 2011), refers to the microfluid system the microfluidic channel in this literature is a nanochannel combining straight line segment with $\frac{1}{4}$ arc of circle. The schematic diagram of the nanochannel used in this research paper for fabrication is shown in Figure 7 below.

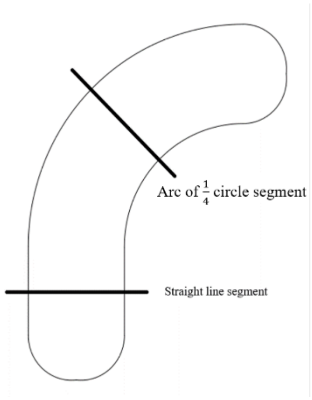

Figure 7 Schematic diagram of nanochannel fabrication

Calculation of Offset Amount, Number of Cutting Passes and Protruding Height Value with the Straight Line Segment Reaching Different Expected Widths and Expected Depths

In order to make the expected width reach 202nm and the expected depth reach 30nm, we use equation (5) $P_{total}= w_e-(2\sqrt{2Rd_e-{d_e}^2})$, about two cutting passes' offset fabrication method of nanochannel trapezium groove, to calculate the number of passes and the number of cutting layers required by us; and the calculated total offset amount is 22nm. Besides, we use equation (7) $H = R - \sqrt{R^2-(\frac{P_n}{2})^2}$ to calculate the protruding height value, which is calculated to be 0.404nm, just lying within the set objective convergence value 0.54nm.

Exploration and Simulation of Cutting Layer of Straight Line Segment

After the paper uses the calculated offset amount of straight line segment, number of offset cutting passes and protruding height value, downward force is substituted to carry out simulation. It is known that the maximum allowable downward force is 137μN. For safety sake, and for prevention of breaking of the probe for being fatigue after cutting for multiple times, we set the least safety coefficient to be 1.5. Under the safety coefficient of 1.5, the maximum downward force is 91.33μN, and its depth can reach 23.014nm only. Therefore, for reaching the objective depth at a deeper depth, the number of cutting layers has to be increased.

Using the above calculation method for the number of cutting passes, offset amount and protruding height value after fabrication of the nanochannel of straight line segment to the expected depth and expected width, we can make calculation that when the expected depth is 30nm and the expected width is 202nm, the offset amount is 22nm, the number of cutting passes is two cutting passes, and the protruding height value on the bottom is 0.404nm. The downward force used on the 1st cutting layer is 91.33μN. As known from the simulation results, the cutting depth is 23.014nm only. Therefore, the paper adds one more cutting layer. On the 2nd cutting layer, the downward force at the 1st cutting pass is 34.92μN; and the downward force at the 2nd cutting pass is 19.88μN. The simulated depth is 30nm; width is 202nm; offset amount is 22nm, and the protruding height value on the bottom is 0.404nm. The simulation results are shown in Table 1 as well as Figure 9.

Table 1 Simulation data of straight line segment at the 2nd cutting pass for the expected width 202nm and the expected depth 30nm

No. of cutting layers	Downward force (μN)	Cutting pass	Simulated cutting depth (nm)	Offset amount (nm)	Protruding height value on the bottom calculated by CAD (nm)	SDFE value ($\mu N\cdot nm/nm^3$)	Removed volume (nm^3)	Width of opening (nm)
1st cutting layer	91.33	1st cutting pass	23.014	22.00	0.404	0.01775	118415.13	181.682
	20.94	2nd cutting pass	23.014			0.01775	27143.57	
2nd cutting layer	34.92	1st cutting pass	30.012	22.00	0.404	0.01775	59099.491	202.001
	19.88	2nd cutting pass	30.012			0.01775	33623.76	

Establishment of Simulation Model of Nanochannel that Integrates Straight Line Segment with Arc Segment Fabrication to the Expected Depth and Expected Width

As mentioned above, the nanochannel

integrates straight line segment with $\frac{1}{4}$ arc segment fabrication to the expected depth and expected width. Its process is that straight line segment is fabricated first, and arc segment is fabricated later. In the integrated fabrication process, since the fabrication from straight line segment fabrication to arc segment fabrication is continuous, the downward force, offset amount, the number of cutting passes and the number of cutting layers used for an ideal curve segment fabrication at each cutting pass are the same as those of straight line segment. When the cutting tool enters the arc segment from the straight line segment, the position of the point of the arc has to be decided first. Therefore, the point of an ideal arc segment at each cutting pass has to be derived first.

Thus, we have to obtain a near arc of $\frac{1}{4}$ circle from different ideal arcs. The method of obtaining the line segments of these near-arcs is through chord height tolerance equation, to make the chord height tolerance less than 0.5nm. Therefore, the next section will explain the establishment process of the coordinates for the arc of a fabricated ideal arc, and the establishment process of the near arc of $\frac{1}{4}$ circle line segment of tiny straight line segments. After that, the paper establishes the AFM-measured cross-section to carry out verification of the simulation results and AFM fabrication experiment.

Calculation of the Coordinates of Ideal Arc at the 1st Cutting Pass and the 2nd Cutting Pass

When calculating the coordinates of an ideal arc segment at the 1st cutting pass, we firstly take equation (12) $L_i^{Arc} = 2\sqrt{r-(r-d_{all\ max})^2}$. Here, $d_{all\ max}$ is supposed to be 0.5nm; r is 400nm; and the obtained L_i^{Arc} is 31.417nm. After the length L_i^{Arc} of tiny straight line segment is obtained, the path starts from the initial point $P(x_1, y_1)$. The length of tiny straight line segment is used to calculate the point of subsequent intersection with the arc of ¼ circle. After repetition of the above calculation method, we can obtain 19 tiny straight line segments of intersection points between the tiny straight line segment L_i^{Arc}=31.417nm and the arc of ¼ circle.

But the length of the last tiny straight line segment L_f^{Arc} of the end point $P(x_2, y_2)$ of the arc of ¼ circle might be smaller than our previously calculated length of tiny straight line segment L_i^{Arc}=31.417nm. Therefore, we further substitute the known value of L_f^{Arc} and the known r=400nm in equation $d_{f\ max} = r - \sqrt{r-(\frac{L_f^{Arc}}{2})^2}$ in order to further calculate the chord height tolerance $d_{f\ max}$ of the last tiny straight line segment L_f^{Arc}, which is calculated to be 0.308nm. This value is smaller than the chord height tolerance 0.5nm set by us. Finally, check whether the chord height tolerances of different tiny straight line segments are smaller than or equal to the size of chord height tolerance set by us.

Then, use calculation method of different tiny straight line segments at the 2nd two cutting passes. Since the offset amount at both the 1st cutting pass and the 2nd cutting pass is 22nm, the 2nd cutting pass' r=400-22=378nm and $d_{all\ max}$ = 0.5nm, and the tiny straight line segment at the 2nd cutting pass can be obtained, with L_{i2}^{Arc}=29.68nm. The last tiny straight line segment is L_{f2}^{Arc}=26.386nm; and the chord height tolerance $d_{f2\ max}$ of the last tiny straight line segment is 0.218nm, which is smaller than 0.5nm. Therefore, at the 2nd cutting pass, there are also 20 tiny straight line segments connecting with the arc of ¼ circle.

Establishment of Line Segment of a Near Arc of $\frac{1}{4}$ circle of Tiny Straight Lines

Since AFM cannot carry out arc fabrication, we can only use tiny straight line segment to replace arc segment. But the smallest resolution achieved in fabrication by AFM machine is up to 1nm only. Since the coordinates of the tiny straight line segments of the line segment of the near arc of $\frac{1}{4}$ circle obtained above have decimals, they are thus rounded up to take their integer values for precision up to 1nm. Then, the integer coordinates of the tiny straight line segments intersecting with the arc of ¼ circle are adopted to redraw a diagram of coordinates of the various tiny straight line segments of a near-arc segment. Figure 8 below shows the coordinates of a near arc line segment with tiny straight line segments at the 1st cutting pass and the 2nd cutting pass after integers of coordinates are taken.

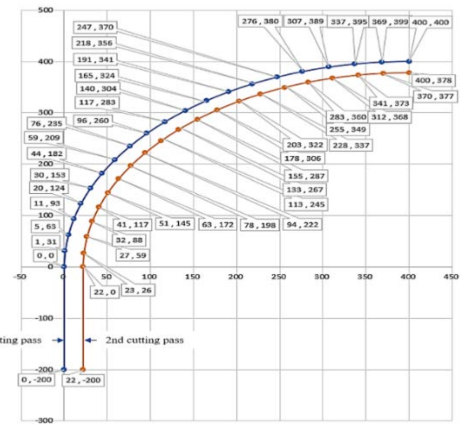

Figure 8 Coordinates of the tiny straight line segments of a near arc line segment at the 1st cutting pass and the 2nd cutting pass after integers of coordinates are taken

Measured Cross-Section and Offset Amount in AFM Fabrication Experiment

Regarding the measured cross-section in AFM fabrication experiment, according to the calculation steps mentioned in before, we take a measured cross-section on a straight line segment, and two measured cross-sections on an arc segment, as shown in Figure 9 below. After calculation, the straight line equations of the measured cross-sections in proper order are: the equation of the first measured cross-section of straight line segment, being y_1 = -150; and the equations of two other measured cross-sections of the arc segment are: the equation of the second measured cross-section, being y_2 = -0.5786x + 243; and the equation of the third measured cross-section, being y_3 = -2.2222x + 880. The offset amount of the first measured cross-section of its straight line segment is 22nm; the offset amount of the second measured cross-sections of the arc segment is 21.954nm; and the offset amount of the third measured cross-sections of the arc segment is 21.931nm. Figure 9 is the diagram of the resulted cross-sections of the measured cross-sections.

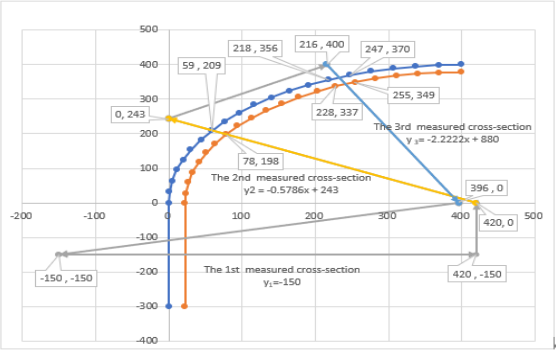

Figure 9 Diagram of the resulted cross-sections of the measured cross-sections

After the above acquisition of the offset amounts of different measured cross-sections, we can start to verify the simulation results and experimental results of the nanochannel that integrates straight line segment with arc of $\frac{1}{4}$ circle segment fabrication to the expected depth and expected width.

Verification of Measurement of Simulation Results and AFM Fabrication Experimental Results of Fabrication to the Expected Depth 30nm and the Expected width 202nm for Two Cutting Passes

After achieving the equations and offset amounts of different measured cross-sections, we start carrying out simulation of the nanochannel that integrates straight line segment with arc of $\frac{1}{4}$ curcle segment fabrication to the expected depth and expected width; and simulated calculation is made for the width of opening, depth and protruding height value on different cutting layers at different cutting passes. SDFE method is also used to calculate the downward force on two cutting layers at the 1st cutting pass and the 2nd cutting pass. After that, we carry out verification of AFM experiment. The comparative results between the simulation results and the measurement results in AFM fabrication experiment are shown in Table 2 and Table 3 below.

Table 2 shows the comparison between the simulation results and the AFM experimental results of cutting on the 1st cutting layer. As seen from Table 2, under different downward forces on the 1st cutting layer at two cutting passes, the difference between the experimental cutting depth and the simulated cutting depth for the three measured cross-sections are all less than 0.1%; and the difference between the experimental width of opening and the simulated width of opening for the three measured cross-sections are all less than 0.02nm; and the experimental and simulated protruding height values on the bottom are also quite close.

Table 2 Comparison between simulation results and experimental results on the 1st cutting layer at two cutting passes for the expected depth 30nm and expected width 202nm

1st cutting layer	Downward force (μN)	Cutting pass	Experimental cutting depth (nm)	Simulated cutting depth (nm)	Difference in cutting depth (nm)	Offset amount (nm)	Experimental protruding height value on the bottom (nm)	Simulated protruding height value on the bottom (nm)	Experimental width of opening (nm)	Simulated width of opening (nm)	SDFE value ($\mu N\cdot m/m^2$)	Difference in width of opening (%)
1st measured cross-section (straight line segment)	91.33	1st cutting pass	20.033(1)	23.014(1)	0.082%	22	0.413(1)	0.404(1)	181.705	181.682	0.01775	0.013%
	20.94	2nd cutting pass	20.033(2)	23.014(2)	0.082%		0.413(2)	0.404(2)				
2nd measured cross-section (circular segment)	91.33	1st cutting pass	20.034(1)	23.014(1)	0.087%	21.954	0.408(1)	0.399(1)	181.667	181.647	0.01775	0.011%
	20.94	2nd cutting pass	20.040(2)	23.021(2)	0.083%		0.414(2)	0.405(2)				
3rd measured cross-section (circular segment)	91.33	1st cutting pass	20.034(1)	23.014(1)	0.087%	21.931	0.406(1)	0.397(1)	181.648	181.627	0.01775	0.012%
	20.94	2nd cutting pass	20.042(2)	23.023(2)	0.082%		0.415(2)	0.406(2)				

Remarks: Cutting depth (1) represents the cutting depth at the 1st cutting pass.
Cutting depth (2) represents the cutting depth at the 2nd cutting pass.
Protruding height value (1) represents the protruding height value from the point of protruding height between the 1st cutting pass and the 2nd cutting pass to the bottom at the 1st cutting pass.
Protruding height value (2) represents the protruding height value from the point of protruding height between the 1st cutting pass and the 2nd cutting pass to the bottom at the 2nd cutting pass.

Table 3 Comparison between simulation results and experimental results on the 2nd cutting layer at two cutting pass for the expected depth 30nm and the expected width 202nm

2nd cutting layer	Downward force (μN)	Cutting pass	Experimental cutting depth (nm)	Simulated cutting depth (nm)	Difference in cutting depth (nm)	Offset amount (nm)	Experimental protruding height value on the bottom (nm)	Simulated protruding height value on the bottom (nm)	Experimental width of opening (nm)	Simulated width of opening (nm)	SDFE value ($\mu N\cdot m/m^2$)	Difference in width of opening (%)
1st measured cross-section (straight line segment)	34.94	1st cutting pass	30.035(1)	30.012(1)	0.077%	22	0.413(1)	0.404(1)	202.061	202.032	0.01775	0.014%
	19.88	2nd cutting pass	30.035(2)	30.012(2)	0.077%		0.413(2)	0.404(2)				
2nd measured cross-section (circular segment)	34.94	1st cutting pass	30.036(1)	30.012(1)	0.080%	21.954	0.408(1)	0.399(1)	202.017	201.995	0.01775	0.011%
	19.88	2nd cutting pass	30.042(2)	30.019(2)	0.077%		0.415(2)	0.406(2)				
3rd measured cross-section (circular segment)	34.94	1st cutting pass	30.036(1)	30.012(1)	0.080%	21.931	0.406(1)	0.397(1)	201.994	201.973	0.01775	0.010%
	19.88	2nd cutting pass	30.044(2)	30.021(2)	0.077%		0.414(2)	0.405(2)				

Remarks: The same as Table 2.

As seen from the results of Table 3, on the 2nd cutting layer of the three measured cross-sections, the simulated cutting depths and width of opening as well as the AFM experimental depths and widths of openings are all quite close to the expected depth 30nm and the expected width 202nm. Besides, as seen from Table 3, the difference in depth of both simulation result and experimental result is less than 0.1%; and the difference in width of opening of both simulation result and experimental result is less than 0.02%; and both their protruding height values on the bottom are also quite close, and also less than the objective convergence value 0.54nm. Therefore, it is proved that the paper's simulation method and AFM fabrication experimental method of nanochannel that integrates straight line segment with arc segment fabrication to the expected depth and expected width is feasible. The diagrams below show the part of measurement results of AFM experiments of three measured cross-sections, as shown in the figures from Figure 10 to Figure 11. These figures prove that the experimental data shown in Table 2 and Table 3 above are acquired in AFM experiments.

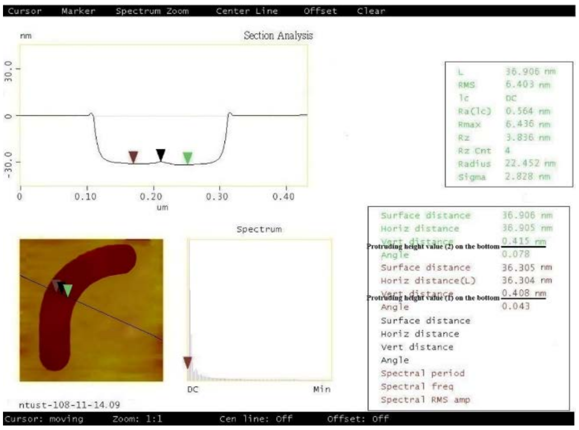

Figure 10 Diagram of experimental measurement of the protruding height value on the bottom of the 2nd measured cross-section (arc segment) on the 2nd cutting layer at two cutting passes for the expected depth 30nm and the expected width 202nm

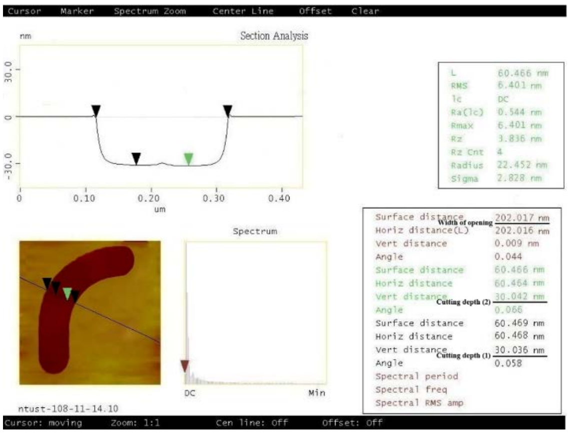

Figure 11 Diagram of experimental measurement of the width of opening and cutting depth of the 2nd measured cross-section (arc segment) on the 2nd cutting layer at two cutting passes for the expected depth 30nm and the expected width 202nm

CONCLUSION

The paper proposes the simulation model and the AFM fabrication experimental method of nanochannel trapezium groove that integrates straight line segment with arc of $\frac{1}{4}$ circle segment fabrication to different expected depths and expected widths.

In order to verify the comparison between the paper's simulation results and experimental results, the paper takes three measured cross-sections of AFM experiment to carry out experimental measurement. Of them, one measured cross-section is on a straight line segment; one is at the intersection point between ¼-circle arc segment of an arc of ¼-circle; and the last one is formed between the position of around the middle of a certain tiny straight line segment of an arc of ¼-circle at the 1st cutting pass and the center of an arc of ¼-circle. The 3rd measured cross-section would intersect with a certain tiny straight line segment at the 2nd cutting pass. The paper also derives equations for these three measured cross-sections. Finally, we carry out comparison between the simulation results and experimental results after integrating straight line segment fabrication with arc of $\frac{1}{4}$ circle segment fabrication of nanochannel trapezium groove to the expected depth and expected width, as established by the paper.

From the comparative results between them, it can be seen that on the 2nd cutting layer of the three measured cross-sections, the simulated depths and widths of openings as well as the AFM experimental depths and widths of openings are all quite close to the expected depth 30nm and the expected width 202nm. Besides, as seen from these comparative results, the difference in depth of both the simulation result and the experimental result is less than 0.1%; and their difference in width of opening are both less than 0.02%; and both their protruding height values are also quite close and less than the objective convergence value 0.54nm. Therefore, it is proved that the paper's simulated calculation method and AFM fabrication experimental method of nanochannel that integrate straight line segment with arc segment fabrication to the expected depth and expected width are feasible.

REFERENCES

Cardoso, V. F., Miranda, D., Botelhoc, G., Minasb, G. and Lanceros-Méndeza, S., "Highly effective clean-up of magnetic nanoparticles using microfluidic technology", Sensors and Actuators B, Vol. 255, pp. 2384–2391 (2018).

Fang, T. H., Weng, C. I. and Chang, J. G., "Fabrication Characterization of Nano-lithography Process by Using Atomic Force Microscopy", Nanotechnology, Vol. 11, No. 5, pp. 181-187 (2000).

Lübben, J. F. and Johannsmann, D., "Nanoscale High-frequency Contact Mechanics Using an AFM Tip and a Quartz Crystal Resonator", Langmuir, Vol. 20, No. 9, pp. 3698-3703 (2004).

Lin, Z. C. and Hsu, Y. C., "A calculating method for the fewest cutting passes on sapphire substrate at a certain depth using specific down force energy with an AFM probe", Journal of Materials Processing Technology, Vol. 212, pp. 2321-2331 (2012).

Nanjo, H., Nony, L., Yoneya, M. and Aime, J. P., "Simulation of Section Curve by Phase Constant Dynamic Mode Atomic Force Microscopy in Non-contact Situation", Applied Surface Science, Vol. 210, No. 1, pp. 49-53 (2003).

Schumacher, H. W., Keyser, U. F. and Zeitler, U., "Controlled mechanical AFM fabrication of two-dimensional electron systems: Fabrication of a single-electron transistor", Physica E., Vol. 6, pp. 860-863 (2000).

Tseng, A. A., "A comparison study of scratch and wear properties using atomic force microscopy", J. Applied Surface Science, Vol. 256, Issue 13, pp. 4246- 4252 (2010).

Teerasong, S. and McClain, R., "A Student-Made Microfluidic Device for Electrophoretic Separation of Food Dyes", Journal of Chemical Education, Vol. 88, pp.465-467(2011)

Wang, Z. Q., Jiao, N. D., Tung, S. and Dong, Z. L., "Research on the atomic force microscopy-based fabrication of nanochannels on silicon oxide surfaces", Chinese Science Bulletin, Vol. 55, No. 30, pp. 3466-3471 (2010).

Yeh, S. S. and Hsu, P. L., "Adaptive-feedrate Interpolation for Parametric Curves with a Confined Error" Computer-Aided Design, Vol. 34, pp. 229-237 (2002).

Yongda, Y., Tao, S., Liang, Y. C. and Shen, D., "Investigation on AFM based micro/nano CNC fabrication system", International Journal of Machine Tools and Manufacture, Vol. 47, No. 11, pp.1651-1659 (2007).

加工直線段連結圓弧之奈米流道到預定寬度及預定深度之模擬模式和公式及原子力顯微鏡加工實驗驗證

林榮慶 秦英傑
國立台灣科技大學 機械工程系

摘要

本文提出加工直線段連結$\frac{1}{4}$圓弧之奈米流道梯型凹槽到預定寬度及預定深度的模擬模式及公式，和用模擬模式所得的探針總偏移量，各切削層的切削道次及兩切削道次間的探針偏移量、底部凸起公式，及各切削層的各切削道次的下壓力，和近似$\frac{1}{4}$圓弧的各微小線段的數目及各微小線段的長度，去進行原子力顯微鏡(AFM)實驗加工到預定寬度及預訂深度的整合直線段加工及$\frac{1}{4}$圓弧加工的奈米流道梯型凹槽。最後並量測 AFM 實驗加工所得之結果，驗證本文所提出的模擬模式及公式為合理可接受。本文並推導出進行量測時，針對近似於$\frac{1}{4}$圓弧曲線的微小線段量測斷面所需的直線方程式，以及量測斷面的方法。綜上所述，本文所提出的上述模擬模式及公式，和 AFM 實驗及量測方法具有學術創新性及應用價值。